A Passive-Based Force Reflecting Algorithm for a Piezo-Actuated Macro-Micro Telemanipulation System

M. Zareinejad [a] *, Saeed Shiry Ghidary [b] and S. M. Rezaei [c]

[a] Department of Engineering, Islamic Azad University of. Islamshahr (IAUI), Islamshahr, Tehran, Iran
[b] Department of Computer Engineering, Amirkabir University of Technology, Tehran, Iran
[c] Department of Mechanical Engineering, Amirkabir University of Technology, Tehran, Iran

Received 20 April 2009; revised 1 November 2009; accepted 12 November 2009

Abstract

Piezoelectric actuators are widely used in micro manipulation applications. However hysteresis nonlinearity limits accuracy of these actuators. This paper presents a novel approach utilizing a piezoelectric nano-stage as slave manipulator of a teleoperation system. The Prandtl-Ishlinskii (PI) model is used to model actuator hysteresis in feedforward scheme to cancel out this nonlinearity. A passive coordination control which uses the new outputs to state synchronize the master and slave robots in free motion is extended to achieve position coordination in contact tasks. The proposed approach uses force feedback using a passivity of the systems and Lyapunov stability methods; the asymptotic stability of force reflecting teleoperation with communication delay and position/force scaling is proven. Performance of the proposed controllers is verified through experiments.

Keywords: Telemanipulation, Passivity control, Piezo-electric actuators, Passive coordination control.

---

1. Introduction

Teleanipulation is defined as the idea of a user interacting with and manipulating a remote environment and has led to wide applications ranging from space-based robotics to telesurgery [1]. Besides several applications of teleoperation systems, there is a new application area which is called Macro-micro teleoperation. Man has restriction to sense or manipulate micro objects directly. Macro-micro teleoperation can enable human to manipulate tasks in micro world. In this paper, a piezoelectric-actuated stage was used as the slave manipulator of a macro–micro teleoperation system. A piezoelectric actuator is an excellent choice as a micro positioning actuator because of its high resolution, fast response and capability of producing high forces.

The hysteresis effect of piezoelectric actuators, which is realized in their response to an applied electric field, is the main setback in precise position control. In this study, a Modified Prandtl–Ishlinskii (PI) model is applied and its inverse is used to cancel out the hysteresis effect. Hysteresis-compensated model can be considered as a second order linear system [2].

One of the challenges associated with micro-teleoperation is the scaling between the human hand and micro parts. Fine motion control in teleoperation is generally achieved through position control with de-amplification from the master to the slave. Higher transparency is accomplished by tracking of scaled force of slave on master side. A method has been proposed to derive scaling factors based on Llewellyn's criteria [3]. However, it has been tested only on virtual environments and no method to tune the gains of the controller has ever been provided. A discrete time sliding mode controller has also been proposed based on Lyapunov theory for piezo-actuated teleoperation system [4]. However, it assumes that time delay is negligible. It has been recognized that the presence of time delay is one of the most important barriers in teleoperation systems. This problem is mainly due to the distance separating the master from the slave site.

There are many control schemes proposed for dealing with the time delay in teleoperation systems [5]. Scattering transformation and wave variables guarantee stability by making the communication channel a passive loss-less transmission line [6, 7].

In this paper, the control scheme proposed in [9, 10], is extended for time delayed bilateral scaled teleoperation system. This framework provides scaled-down position coordination in both cases of free and constrained motions. Moreover, higher transparency can be achieved by tracking

---

* Corresponding author. E-mail: mzare@aut.ac.ir

of scaled-up force on the master side. To deal with the noise of numerical differentiation method, velocity is estimated by a linear observer. Comprehensible structure of the controller presents a low cost and easily- implemented control framework.

2. Synchronization Architecture for Bilateral Teleoperation System

2.1. Dynamics of Teleoperation

The Euler-Lagrange equations of motion for an n-degree-of freedom mechanical system is given as[11]:

$$M(q)\ddot{q} + C(q,\dot{q})\dot{q} + g(q) = \tau \tag{1}$$

Where $q \in R^n$ the vector of generalized configuration is coordinates, $\tau \in R^n$ is the vector of generalized forces acting on the system, $M(q)$ is the $n \times n$ symmetric, positive definite inertia matrix, $C(q,\dot{q})$ is the matrix of Coriolis and centripetal torques and $g(q)$ is the vector of gravitational torques. The above equation of motion exhibits certain fundamental properties due to its Lagrangian dynamic structure. Skew-symmetry of the matrix $\dot{M} - 2C$ is the most important property [9].

One can obtain passivity of the Euler-Lagrange dynamics from input τ to output $q$using the skew-symmetry property.

More generally, with a different choice of output and a preliminary feedback control which is called *Feedback Passivation* [9, 12] one can induce passivity in a Lagrangian system. To this end, a Preliminary control input is chosen as:

$$\tau = -M(q)\lambda\ddot{q} + C(q,\dot{q})\lambda\dot{q} + g(q) + u \tag{2}$$

where λ is a positive diagonal matrix and u is an additional control input. Setting $r = \dot{q} + \lambda q$, the new system can be written as follows:

$$\dot{q} = -\lambda q + r \tag{3}$$

$$M(q)\dot{r} + C(q,\dot{q})r = u \tag{4}$$

which is in the form of:

$$\dot{x} = f(x) + g(x)u \tag{5}$$

with state vector $x = (q,r)$ and vector fields f and g is given by:

$$f(x) = \begin{pmatrix} -\lambda q + r \\ -M^{-1}(q) + C(q,\dot{q})r \end{pmatrix} \tag{6}$$

$$g(x) = \begin{pmatrix} 0 \\ M^{-1}(q) \end{pmatrix} \tag{7}$$

Passivity of the above system can be proved easily using the skew-symmetry property, and considering input u, output $y = h(x) = r$, and storage function $V(x) = r^T M(q) r$.

Assuming the absence of friction and other disturbances, the master and slave robot dynamics with n-degree-of-freedom are described as:

$$M_m(q_m)\ddot{q}_m + C_m(q_m,\dot{q}_m)\dot{q}_m + g_m(q_m) = \tau_m + F_{op} \tag{8}$$

$$M_s(q_s)\ddot{q}_s + C_s(q_s,\dot{q}_s)\dot{q}_s + g_s(q_s) = \tau_s + F_{env} \tag{9}$$

The subscript “m” and “s” denote the master and slave indexes, respectively. τ_m, τ_s are the input torque vectors. F_{op} is the operational force vectors applied to the master robot by human operator, F_{env} is the environmental force vectors applied to the environment by the slave robot.

Furthermore, some assumptions are considered for stability analysis as follows:

Assumption 1: The communication delay between master and slave robot are constant delays as T. For the sake of simplicity, it is supposed that the forward and backward communication delays are equal. However, the following stability results are valid for asymmetric time delay.

Assumption 2: All signals belong to L_{2e}.

Assumption 3: Under an appropriate definition of the matrix$C$, the matrix $\dot{M} - 2C$ is skew symmetric.

2.2. Control Design

To achieve the synchronized teleoperation system, the master and slave robot inputs are given as:

$$\tau_m = F_m - M_m(q_m)\lambda\dot{q}_{m(t)} - C_m(q_m,\dot{q}_m)\lambda q_m(t) + g_m \tag{10}$$

$$\tau_s = F_s - M_s(q_s)\lambda\dot{q}_s(t) - C_s(q_s,\dot{q}_s)\lambda q_s(t) + g_s \tag{11}$$

where λ is a constant positive definite matrix. F_m and F_s are the additional inputs required for synchronized control.

The position error-based control approach used in [9-10] ensures position coordination just in free motion. Therefore, by considering force feedback in the control, the proposed control law can be written as follows:

$$F_m = K\left(K_p r_s(t-T) - r_m(t)\right) + K_m\left(K_f F_{env}(t-T) - F_{op}(t)\right) \tag{12}$$

$$F_s = K\left(r_m(t-T) - K_p r_s(t)\right) + K_s\left(F_{op}(t-T) - K_f F_{env}(t)\right) \tag{13}$$

where K_p and K_f are position and force scaling factors, respectively. K is a positive definite diagonal control gain matrix and K_m and K_s are positive control gains for the master and slave robots, respectively. $r_m(t)$ and $r_s(t)$ are the new outputs of the master and slave robots, respectively. $r_i(t)$ is computed as $r_i(t) = \lambda q_i(t) + \dot{q}_i(t)$. Comparing to [9-10], a force compensation term is added to control laws.

2.3. Stability Analysis

Assumption 3: The human operator and the environment can be modeled as passive systems, respectively, as follows [10]:

$$F_{op}(t-T) = -\alpha_m r_m(t-T) \quad \alpha_m > 0 \tag{14}$$

$$F_{env}(t-T) = -\alpha_s r_s(t-T) \quad \alpha_s > 0 \tag{15}$$

Definition1: the coordination errors between the master and slave robots are defined as:

$$\begin{cases} e_s = K_p q_s(t-T_s) - q_m(t) \\ e_m = q_m(t-T_m) - K_p q_s(t) \end{cases} \tag{16}$$

Theorem 1. Consider the nonlinear bilateral teleoperator described by (8)-(13). In the presence of constant communication delays, all signals in the system are ultimately bounded.

Proof: Consider a positive semi-definite storage functional V_{ms} for the system as:

$$\begin{aligned} V_{ms}(t) = {} & r_m^T(t)M_m(q_m)r_m(t) \\ & + K_p r_s^T(t)M_s(q_s)r_s(t) \\ & + e_m^T(t)\lambda K e_m(t) + e_s^T(t)\lambda K e_s(t) \\ & + 2K_p(K_f K_s + 1)\int_0^t \{F_{env}^T(\tau)r_s(\tau)\}d\tau \\ & - 2(K_m + 1)\int_0^t \{F_{op}^T(\tau)r_m(\tau)\}d\tau \end{aligned} \tag{17}$$

The derivative of $V_{ms}(t)$is given as:

$$\begin{aligned} \dot{V}_{ms}(t) = {} & 2r_m^T(-C_m r_m + F_m + F_{op}) \\ & + r_m^T \dot{M}_m r_m + 2K_p r_s^T((-C_s r_s + F_s - F_{env}) + K_p r_s^T \dot{M}_s r_s \\ & + r_m^T K r_m - K_p r_s^T(t-T)K r_s(t-T) + K_p r_s^T K r_s \\ & - r_m^T(t-T)K r_m(t-T) + 2\left(e_m^T \lambda K e_m + K_p e_s^T \lambda K e_s\right) \\ & +2K_p\left(K_f K_s + 1\right)r_s^T F_{env} - 2(K_m + 1)r_m^T F_{op} \end{aligned}$$

Using the values of r_m, r_s and replacing F_m, F_s and considering assumptions 1-3, $\dot{V}_{ms}(t)$ reduces to:

$$\begin{aligned} \dot{V}_{ms}(t) = {} & \underbrace{-\dot{e}_m^T K \dot{e}_m - e_m^T \lambda K e_m - \dot{e}_s^T K_p K \dot{e}_s - e_s^T \lambda K_p K e_s}_{\dot{V}_{ms1}(t) \leq 0} \\ & - \underbrace{(2r_s^T K_p K_s \alpha_m r_m(t-T) + 2r_m^T K_m K_f \alpha_s r_s(t-T))}_{\dot{V}_{ms2}(t)} \end{aligned}$$

Considering these two facts:

$$\begin{aligned} & 2r_s^T K_p K_s \alpha_m r_m(t-T) \\ & \qquad \leq r_s^T(t)K_p K_s \alpha_m r_s(t) \\ & \qquad + r_s^T(t)K_p K_s \alpha_m r_s(t) \end{aligned} \tag{18}$$

and

$$\begin{aligned} & 2r_m^T K_m K_f \alpha_s r_s(t-T) \\ & \qquad \leq r_m^T(t)K_m K_f \alpha_s r_m(t) \\ & \qquad + r_s^T(t-T)K_m K_f \alpha_s r_s(t-T) \end{aligned} \tag{19}$$

$\dot{\mathrm{V}}_{\mathrm{ms}\,2}(\mathrm{t})$ can be rewritten as following:

$$\begin{aligned} & \dot{V}_{ms2} \leq \\ & -\left(r_m^T(t)K_p K_s \alpha_m r_m(t)\right) - \left(r_s^T(t-T)K_p K_s \alpha_m r_s(t-T)\right) \\ & -\left(r_m^T(t)K_p K_s \alpha_s r_m(t)\right) - (r_s^T(t)K_p K_s \alpha_s r_s(t)) \end{aligned}$$

Consequently:

$$\dot{V}_{ms}(t) = \dot{V}_{ms1} + \dot{V}_{ms2} \leq 0$$

As $\dot{V}_{ms}(t)$is negative semi-definite, therefore, $\lim_{t\to\infty} V_{ms}$exists and is finite. Following the proof of Theorem 2.1 [10], it can be shown that all signals are bounded and $\lim_{t\to\infty}(e_m, \dot{e}_m, e_s and\ \dot{e}_s) = 0$

3. Observer-Controller Scheme

Industrial robots are often equipped with very accurate sensors to measure position, whereas they lack sensors for measuring of velocity for considerations of cost, volume, and weight. An alternative method is to obtain an estimation of velocity from position measurements using a simple numerical differentiation method.

This is, however, a very noise sensitive approach. A better way to deal with the problem is to use observers to estimate the velocity. Since the master and slave manipulators are linear, a full order state observer is utilized to provide an estimation of internal states through the measurements of some inputs and outputs. Consider the observable system (25) and (26) described in state space

$$\dot{x} = Ax + Bu \tag{20}$$

$$y = Cx \tag{21}$$

where $x \epsilon R^n$denotes the state of the system, y is the measured output, u is the control input $A \in R^{n\times n}$ $B \in R^{n\times n}$, contain system's parameters and $C \in R^{m\times n}$is used to select the m outputs [11]. The state x of (25) can be estimated by means of a full order linear observer is designed as follows:

$$\dot{\hat{x}} = A\hat{x} + Bu + L(y - \hat{y}) \tag{22}$$

$$\hat{y} = C\hat{x} \tag{23}$$

where $\hat{x}\ \varepsilon\ R^n$, $\hat{y}$ are the estimated state and the estimated output respectively. $L \varepsilon\ R^n$ is the observer gain vector that can be chosen such that the polynomial characteristic of

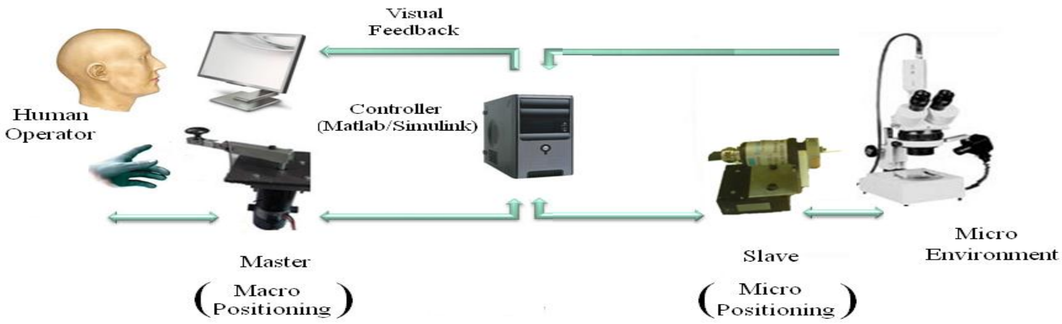

Fig. 1. Micro telemanipulation setup.

$(A - LC)$ is Hurwitz. If 22 Subtracted from 20 and by introducing the observer state error $\tilde{e} = x - \hat{x}$, one can obtain:

$$\dot{\tilde{e}} = (A - LC)\tilde{e} \triangleq \bar{A}\tilde{e} \tag{24}$$

To prove that the estimation error tends to zero asymptotically, let us consider (24) together with the following YKP equation

$$P\bar{A} + \bar{A}^T P = -Q$$

where P and Q are positive definite symmetric matrices, with the Lyapunov candidate function $V_o = \frac{1}{2}\tilde{e}^T P\tilde{e}$ whose time derivative is:

$$\begin{aligned}\dot{V}_o = 2\tilde{e}^T P\dot{\tilde{e}} = 2\tilde{e}^T P\bar{A}\tilde{e} = \tilde{e}^T P\bar{A}\tilde{e} + \tilde{e}^T \bar{A}^T P\tilde{e} \\ = -\tilde{e}^T Q\tilde{e} \le -\lambda_{min}\, Q\|\tilde{e}\|^2\end{aligned} \tag{25}$$

From (25), it is obvious that the estimation error tends asymptotically to zero.

4. Macro-Micro Telemanipulation System

Figure 1 shows the master-slave system for a micro telemanipulation setup. To design an efficient controller for this system, the dynamics equations of motion of the teleoperation system are first derived.

4.1. Dynamic Modeling for the Master Robot

In this research, the master is a 1-DOF manipulator which utilizes a DC servo motor. A load cell is installed on the shaft of the motor to measure the force exerted on the master. The dynamic model of the motor can be considered as follows:

$$\begin{aligned}j_m\ddot{\theta}_m(t) + b_m\dot{\theta}_m(t) + k_m\theta_m(t)(t) \\ = u_m(t) + L_m F_h(t)\end{aligned} \tag{26}$$

where θ_m denote rotation angle, j_m, b_m and k_m are moment of inertia of the rotating system, damping and stiffness, respectively. F_h is the force exerted by human operator and L_m is the effective length between the force and motor shaft. u_m is control signal that is applied to the master robot.

4.2. Dynamic Modeling for the Slave Robot

The slave manipulator consists of a 1-DOF stage actuated by a piezo stack actuator. The hysteresis effect of piezoelectric actuators which is revealed in their response to an applied electric field is the main drawback in precise positioning. Therefore, the development of a dynamic model which describes the hysteresis behavior is highly important to improve the control performance of the piezo-positioning mechanism. In many investigations, a second-order linear dynamics has been utilized for describing the system dynamics. As shown in Figure 2, this model combines mass-spring-damper ratio with a nonlinear hysteresis function appearing in the input excitation to the system. The following equation defines the model:

$$m_s\ddot{x}_s(t) + b_s\dot{x}_s(t) + k_s x_s(t) = H_F\big(v(t)\big) \tag{27}$$

where $\mathrm{x_s}(t)$ is the salve position, $\mathrm{m_s}, \mathrm{b_s}$ and $\mathrm{k_s}$ are mass, viscous coefficient and stiffness respectively.

$H_F\big(v(t)\big)$ denotes the hysteretic relation between input voltage and excitation force. Piezoelectric actuators have very high stiffness, and, consequently, possess very high natural frequency. In low-frequency operations, the effects of actuator damping and inertia could be safely neglected. Hence, the governing equation of motion is reduced to the following static hysteresis relationship between the input voltage and actuator displacement:

$$\begin{aligned}&x(t) = \frac{1}{k_s}H_F\big(v(t)\big) = H_x\big(v(t)\big) \\ &\{m_s\ddot{x}_s(t) \ll b_s\dot{x}_s(t) \ll k_s x_s(t)\}\end{aligned} \tag{28}$$

Equation (28) facilitates the identification of the hysteresis function $H_F\big(v(t)\big)$ between the input voltage and the excitation force. This is performed by first identifying the hysteresis map between the input voltage and the actuator displacement $H_x\big(v(t)\big)$. It is then, scaled up to $\mathrm{k_s}$ to obtain $H_F(v(t))$. To consider interaction with environment, the force F_e exerted by the environment is inserted into the model. Therefore, the dynamic model of the slave manipulator can be written as follows:

$$m_s\ddot{x}_s(t) + b_s\dot{x}_s(t) + k_s x_s(t) = k_s H_x(v(t)) - F_e \qquad (29)$$

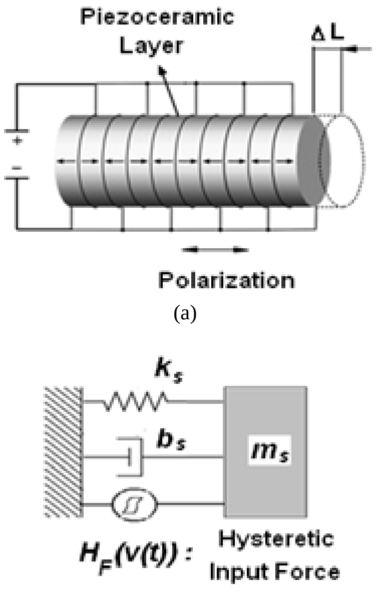

(a)

(b)

Fig.2. (a) Piezoelectric stack actuator; (b) Equivalent dynamic model.

4.3. Hysteresis Modeling

In this paper, Prandtl-Ishlinskii (PI) model is utilized to cancel out hysteresis nonlinearity. It is known that the PI model consists of both play operators and stop operators [6]. Considering the difficulty of the determination of the parameters for PI model, the elementary operators of the simplified PI model are only backlash operators. The hysteresis can be described by a sum of weighted backlash operators with different thresholds and weight values. This model can approximate the hysteresis loop accurately and its inverse could be obtained analytically. Therefore, it facilitates the inverse feedforward control design.

Graphically, the inverse is the reflection of the resultant hysteresis loop about the 45° line. Kuhnen [13] proved that PI and inverse model of PI are Lipschitz continuous and thus input-output stable.

4.4. Feedforward Hysteresis Compensation

The structure of inverse feedforward hysteresis compensation is shown in Figure 3.a. The key idea of an inverse feedforward controller is to cascade the inverse hysteresis operator H_x^{-1} with the actual hysteresis represented by the hysteresis operator H_x. In this manner, an identity mapping between the desired actuator output $x_d(t)$ and actuator response $x(t)$ is obtained (Figure 3.c).

The inverse of PI operator H_x^{-1} uses $x_d(t)$ as input and transforms it into a control input $v_{H_x^{-1}}(t)$ which produces $x(t)$ in the hysteretic system that closely tracks $x_d(t)$.

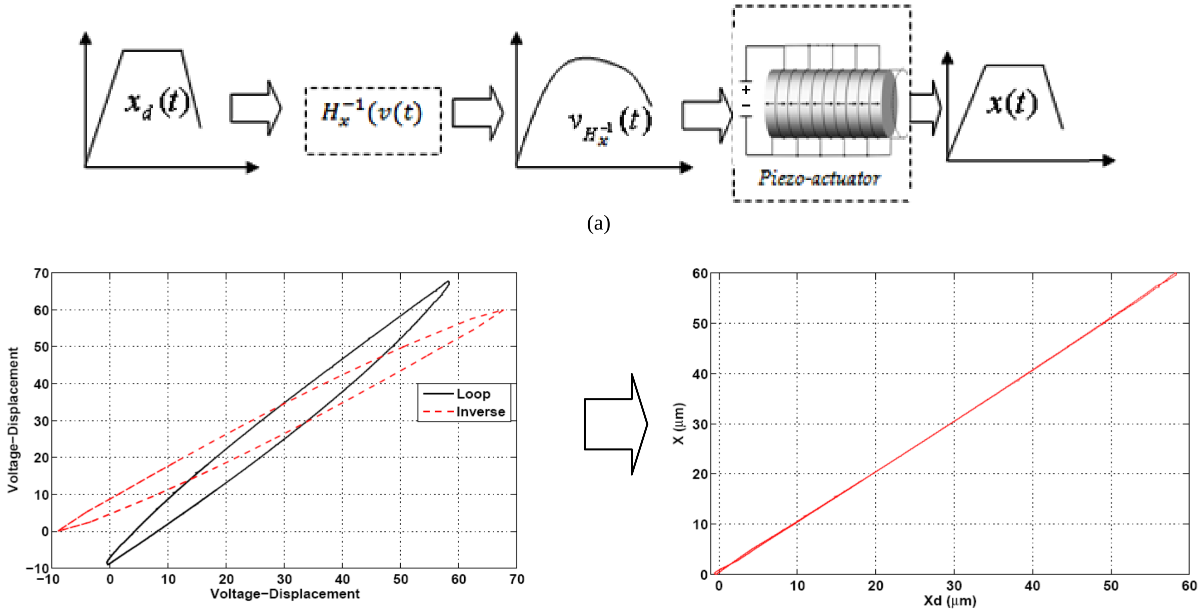

(a)

(b)

(c)

Fig. 3. (a) Inverse Feedforward hysteresis compensation; (b) Hysteresis vs. inverse loop; (c) x_d vs. x after compensation.

5. Experimental Results

In this section, the experimental results of the macro-micro teleoperation system are presented.

5.1. Experimental Setup

As shown in Figure 4, a Physik Instrumente PZT-driven nanopositioning stage (PI 611.1s) with high resolution strain gage position sensor is used as the slave manipulator. The E500 module includes E501 Piezo driver, E503 strain gage amplifier which carry out experimental data. A rigid needle is mounted on the stage. A hi-precision load cell is used to measure environmental force.

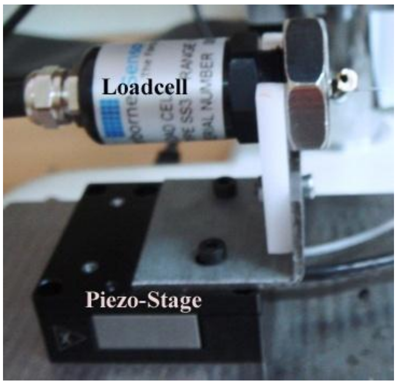

Fig. 4. Nanopositioning stage as the slave robot.

A dSpace1104 board is used as interface element between MATLAB Real Time Workshop and the equipments. The controllers are developed in Simulink and implemented in real time using MATLAB Real-Time Workshop and through Control Desk software. To effectively implement the controller, the sampling frequency is set to $10\,KHz$. The master Manipulator consists of a DC servo motor which is equipped with a high resolution encoder. A load cell is installed on motor shaft to measure force exerted on the master (Figure 5). A Digital Motor Controller is used for driving the DC servomotor.

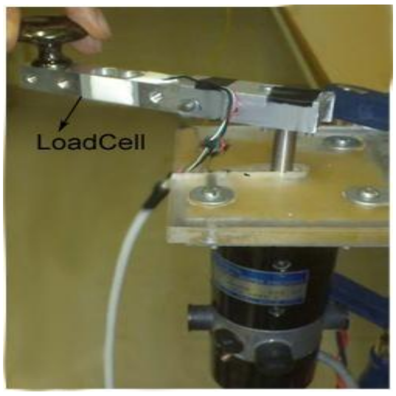

Fig. 5. DC-servo motor as the master manipulator.

5.2. Results

For verification of the proposed controllers, human operator manipulates the master end-effector to generate a desired position trajectory. The human desired trajectory is then transferred to the slave side with position scaling gain $K_P = \frac{1e^{-5}}{2\pi}$ such that with master rotation of 360°, piezo-stage moves 100 μm.

The motion of the slave end-effector contains two stages as follows:

(I) Free motion when the slave end-effector does not contact with the environment.

(II) Interaction stage, when the slave end effector exerts force on the environment. At this stage, the end-effector exerts an interaction force on the external environment and also moves forward. The contact force due to the environment is then transferred to the master side with force reflecting gain $K_f = 100$.

Two experiments were performed. The first one without time delay and the second one with a time delay of $T_1 + T_2 = 0.7$s. In the arranged task, when the slave follows the motion of the master, it contacts an obstacle at time t = 2.5s.

After the contact, the end-effector moves forward. It, then, keeps the master position for some seconds before returning to the home position. This task is repeated twice. Figure 6 and 7 show the experimental results for position and force tracking without time delay. The proposed scheme shows good tracking performance. In spite of the contact with the environment, the slave side can still track the master desired position (Figure 6) while force reflected back to the master side is increasing (Figure 7).

The controllers are capable of achieving both position/force tracking. Since operator tries to keep master in a fixed position, hand chattering leads to noisy force signal.

Experimental results for position /force tracking under communication time delay are depicted in Figures 8 and 9. T_1 and T_2 were implemented using Simulink time delay. These were set as $T_1 = 0.4$s and T2 = 0.3s, respectively. The slave tracks the master commands and maintains a stable contact with the environment. Moreover, the proposed algorithm provides proper force tracking in contact with the environment.

The amplitude of force in Figures 7 and 9 is not equal because in each experiment, position of the obstacle was different.

6. Conclusion

In this paper, a macro-micro teleoperation was implemented using piezoelectric actuator as the slave manipulator. An inverse model-based feedforward controller was then proposed and implemented to compensate for the hysteresis of piezoelectric actuator.

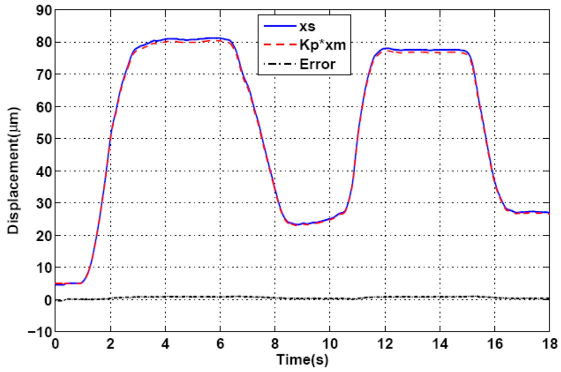

Fig.6. Master/slave position signals without delay.

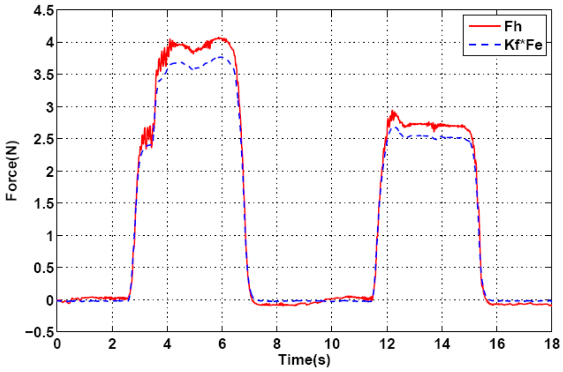

Fig. 7. Master/slave force signals without delay.

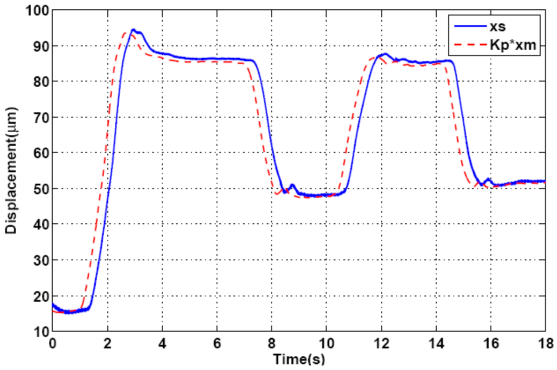

Fig. 8. Master/slave position signals with delay.

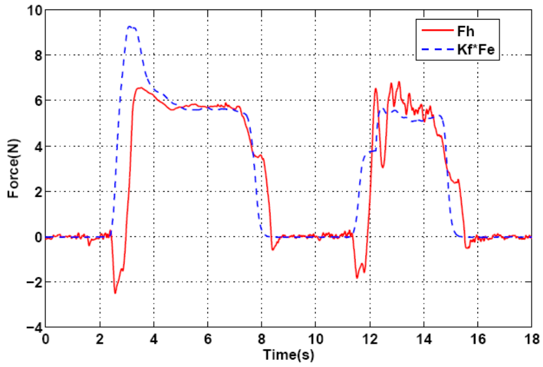

Fig.9. Master/slave force signals with delay.

The proposed control scheme in [9-10], is extended for time delayed bilateral scaled teleoperation system. This framework provides position coordination in both cases of free and contact motions while preserving stability of the teleoperator against time delay.

To deal with position drift in constrained motion, a force Compensation term is also added to the control system. Using the Lyapunov stability method, the proposed control structure is shown to be stable. The experimental results verify the accurate position tracking in free motion and simultaneous position and force tracking in constrained motion.

References

[1] M. Zareinejad, S.M. Rezaei, S.S. Ghidary and A. Abdullah, Development of a piezo-actuated micro-teleoperation system for cell manipulation, International Journal of Medical Robotics and Computer Assisted Surgery, 5: pp. 66–76, 2009.

[2] M. Zareinejad, S.M. Rezaei,H.H. Najafabadi, S.S.Ghidary, A. Abdullah and M. Saadat, Novel multirate control strategy for piezoelectric actuators. Proc. IMechE, Part I: J. Systems and Control Engineering, 223 (5), pp. 673-682, 2009.

[3] S.-G. Kim and M. Sitti, Task-based and stable telenanomanipulation in a nanoscale virtual environment, IEEE Trans. on AutomationScience and Engineering, vol. 3, no. 3, pp. 240–247, July 2006.

[4] S.Khan, A.Sabanovic and A.O.Nergiz, Scaled bilateral teleoperation using discrete-time sliding mode controller, IEEE Trans. on Industrial Electronics, 2009.

[5] P. F. Hokayem and M. W. Spong, Bilateral teleoperation: An historical survey, Automatica, vol. 42, no. 12, pp. 2035-2057, 2006.

[6] R. J. Anderson and M. W. Spong, Bilateral control of teleoperators with time Delay, IEEE Trans. Automat. Control, vol. 34, no. 5, pp. 494- 501, 1989.

[7] G. Niemeyer and J. J. E. Slotine, Stable adaptive teleoperation IEEE J. Oceanic Eng., vol. 16, no. 1, pp. 152 - 162, 1991.

[8] D. Lee and M. W. Spong, Passive bilateral teleoperation with constant time delay, IEEE Trans. Robot, vol. 22, no. 2, pp. 269-281, 2006.

[9] F. Bullo and K. Fujimoto (Eds.), Lecture Notes in Control and Information Sciences, Vol. 366, Springer Verlag, pp. 47-59, 2007.

[10] N. Chopra, M.W. Spong, and R. Lozano, Synchronization of bilateral teleoperators with time Delay, Automatica, vol. 44,Issue 8, pp. 2142-2148, 2008.

[11] R. Ortega, Passivity-based control of euler-lagrange systems: mechanical, electrical and. electromechanical applications. Springer-Verlag, London, 1998.

[12] Sepulchre, M. Jankovi´c, and P. Kokotovi´c. Constructive nonlinear control. Springer-Verlag, London, 1997.

[13] K. Kuhnen and P. Fabio, Modeling, identification and compensation of complex hysteretic nonlinearities: A modified Prandtl-Ishlinskii approach. European journal of control, 2003, pp. 407-421.

[14] T. Kailath, A. H. Sayed and B. Hassibi, Linear Estimation. Prentice Hall; 1st edition, New Jersey, 2000.